# WAVELET-BASED DENOISING AND INDEPENDENT COMPONENT ANALYSIS FOR IMPROVING MULTI-GROUP INFERENCE IN FMRI DATA

*Siddharth Khullar[1,2], Andrew Michael[2], Nicolle Correa[3], Tulay Adali[3], Stefi Baum[1], Vince Calhoun[1,2,3,4]*

1. Chester F. Carlson Center for Imaging Science, Rochester Institute of Technology, Rochester, NY, USA
2. Mind Research Network, Albuquerque, NM, USA
3. University of Maryland, Baltimore County, Baltimore, MD, USA
4. University of New Mexico, Albuquerque, NM, USA

## ABSTRACT

Denoising is amongst the most challenging steps involved in analyzing fMRI data. The conventionally used Gaussian smoothing improves the SNR at the cost of spatial sensitivity and specificity. We briefly describe a 3-D framework for wavelet based fMRI analysis that includes denoising and signal separation followed by a detailed illustration of the benefits and improvements when applied to multi-group (healthy/patient) fMRI studies. We utilize a novel shape metric to highlight the accuracy of the shape of activation regions obtained through different processing frameworks. The proposed algorithm results in higher specificity and increased shape accuracy which in turn is likely to be more sensitive to important differences in the patient and control group.

***Index Terms***— fMRI, Wavelets, Denoising, 3-D, Shape metrics

## 1. INTRODUCTION

Pre-processing of fMRI data is a necessary step before applying any signal separation algorithms. Spatial smoothing or spatial denoising is the last step in the so-called 'fMRI pre-processing pipeline' and likely has the most impact on the results. Conventionally, the data is smoothed using a variable size Gaussian smoothing kernel (e.g. $10 \times 10 \times 10$ $mm^3$). This method has long been well-received by the fMRI community as it is computationally less expensive and the resulting data has a good signal-to-noise ratio (SNR). It is integrated with many widely-used software packages such as SPM [1], AFNI [2] and FSL [3]. These packages provide a wide range of pre- and post-processing tools (other than denoising) encouraging their use for integrated fMRI analysis. But, in recent years there have been tremendous advancements and improvements in the field of fMRI pre-processing resulting in a strong shift towards new mathematical models of signal processing.

As the current research continues to advance towards identifying imaging bio-markers for different brain disorders, sensitivity and specificity provided by different methods has gained higher importance.

A relatively recent development in field of image processing is the wavelet transform which simply projects the data in a different space (wavelet domain). This new space is comprised of several representations of the raw data at various scales of frequency and space [4]. Over the past two decades numerous methods in the literature [5-9] utilize the properties of wavelet transforms to better understand the underlying information in BOLD fMRI signals. They have been repeatedly used as a basis in pre-processing applications such as spatial denoising of fMRI data [7, 9, 10] in addition to their utility as a tool for fMRI signal separation [5, 6, 8, 10, 11].

In this paper, we briefly describe a recently proposed framework [10] accompanied by a well detailed description of its application and benefits for analyzing group differences between healthy controls (HC) and schizophrenia patients (SZ). When performing multi-group studies especially those involving patients suffering from disorders such as schizophrenia or bipolar disorder, one needs to take the pre-processing effects on the data into account. The group difference statistics are undoubtedly affected by fMRI spatial pre-processing steps that include smoothing and normalization. As a solution to the denoising problem, we present an alternative smoothing scheme [10] that utilizes wavelets for denoising the fMRI volumes followed by ICA on wavelet-transformed data instead in the spatial domain. The ICA components are then reconstructed using inverse transform to obtain the activation maps in the spatial domain. The reason behind performing ICA in the wavelet domain is coherent with the fact that wavelet coefficients are decorrelated with respect to different spatial frequency bands. This serves as an added benefit for the ICA algorithm who's primary function is to separate the data into maximally independent components. The representation of data in the wavelet space helps in determining better edge-details and accurate contours for the resulting activation regions. In the latter half of this paper, the differences between the proposed framework and the conventional processing scheme (Gaussian smoothing + spatial ICA) are

presented from a perspective of analyzing multi-group differences between HC and SZ. The primary basis for comparison between the aforementioned frameworks is a recently proposed shape validation metric, also described in [10].

This paper is organized as follows: the methodological details including the proposed algorithm are presented in Section 2 followed by illustration of results and discussion of advantages and benefits of the method in Section 3. Finally, conclusions are drawn in Section 4.

## 2. METHODS

### 2.1 Participants

The subjects used in this study consisted of 5 healthy controls, 5 chronic schizophrenia patients, all of whom gave written and informed, IRB approved consent at the Hartford Hospital and were compensated for their participation. Patients were slightly older than controls (SZ age = 39.7 ± 10.1; HC age = 31.2 ± 10.9). More details about the above mentioned data set can found in [12].

### 2.2 Experimental Design

All subjects were scanned twice (two sessions each lasting 8-min) while performing the auditory oddball task (AOD). The AOD task comprises of pressing a button when the subject hears an infrequent sound within a series of regular and different sounds. The stimulus paradigm data acquisition techniques and previously found stimulus-related activation are described more fully elsewhere [13].

### 2.3 Image Acquisition & Pre-processing

All scans were acquired at a single site – Olin Neuropsychiatry Center at the Institute of Living/Hartford hospital on a Siemens Allegra 3T dedicated head scanner. The specifics of the acquisition parameters set for acquiring the functional scans trans-axially with gradient-echo EPI can be found in [12].

The data were preprocessed using the SPM5 software package (http://www.fil.ion.ucl.ac.uk/spm/software/). The data were (a) motion corrected independently of the local signal variations using the INRIalign algorithm [14]; (b) spatially normalized into the MNI space and (c) slightly resampled from 3.75 × 3.75 × 4 $mm^3$ to a voxel size 3 × 3 × 3 $mm^3$ resulting in 53 × 63 × 46 voxels per volume.

### 2.5 Wavelet-based 3-D Denoising and w-ICA

A step-by-step detailed description of the framework used in this paper can be found in [10]. This paper focuses more on its application for comparing analysis methods for multi-group fMRI studies. The first step of the proposed framework is wavelet based 3-D denoising. The fundamental principle of signal estimation [15] behind the proposed methodology was first used for medical image denoising by [7] and has been recently integrated with a signal separation and validation framework for a robust analysis of fMRI [10].

The algorithm commences with the computation of eight wavelet sub-bands through a 3-D stationary wavelet transform. The number of levels is left (2 in this case) as a parameter for the user to decide depending on the quality of denoising required. The seven 3-D detail sub-bands (LLH, LHL, LHH, HLL, HLH, and HHH) are then used as the noisy sub-bands which are denoised using the methodology described in [10]. The first component in the estimator requires the conditional probability distributions of the magnitude of wavelet coefficients (for each sub-band volume) corresponding to the signal and noise. Empirically, these distributions are obtained by utilizing the histogram distributions of signal and noise voxels [10] in that sub-band. The ratio of these distributions is expressed as:

$$\hat{\xi}_k = \frac{\hat{p}_{m_k|\hat{x}_k}(m_k \mid \hat{x}_k = 1)}{\hat{p}_{m_k|\hat{x}_k}(m_k \mid \hat{x}_k = 0)} \tag{1}$$

Where $m_k = |w_k|$ for each $k^{th}$ voxel and any arbitrary sub-band $D$. The conditions $\hat{x}_k = 1$ and $\hat{x}_k = 0$ represent the a priori binary maps for signal and noise respectively. These maps are obtained using a thresholding procedure explained in [7, 10].

The second component required for the estimator is termed as the local spatial activity indicator or the expected value indicator $E_k$. The value of $E_k$ is computed using a 3-D neighborhood kernel of size 3×3×3 and by utilizing the wavelet coefficients from the next higher level $j$+1 to estimate the signal at the current level $j$. This hierarchical scheme is followed until the coarsest level is reached, that is, $j$ = 1. The ratio of the probabilities of local spatial activity for signal to noise is expressed as:

$$\hat{\mu}_k = \frac{\hat{p}(x_k = 1 \mid e_k)}{\hat{p}(x_k = 0 \mid e_k)} = \frac{p(x_k = 1)\, p_{e_k|x_k}(e_k \mid x_k = 1)}{p(x_k = 0)\, p_{e_k|x_k}(e_k \mid x_k = 0)} \tag{2}$$

The above expression is obtained using the Bayes' theorem. A detailed solution can be found in [7, 10]. The expression for the final estimated value of the signal can be written as:

$$\hat{y}_k = \frac{\hat{\xi}_k \hat{\mu}_k}{1 + \hat{\xi}_k \hat{\mu}_k} w_k \tag{3}$$

Each sub-band D corresponds to a denoised estimate $\hat{\mathbf{y}}_k^L$ at level $j$ = 1. The final denoised data $\hat{\mathbf{y}}_k^{\Gamma}$ is in the form of eight 3-D wavelet sub-bands (including the LLL band) at level $j$ = 1. This data is reduced from a 3-D sub-band form to a 2-D sub-band for each axial slice by using wavelet reconstruction filters along the $z$-direction [10] in order to reduce computational complexity in the wavelet-ICA step. ICA is applied on the denoised wavelet coefficients with an order = 20 components, using the GIFT toolbox[12].

Fig. 1 illustrates a detailed block diagram of the proposed fMRI processing framework that also includes the

validation stage comprising of a shape metric. The results of the shape metric are presented to highlight the advantages of our proposed wavelet-based scheme over conventionally used methods.

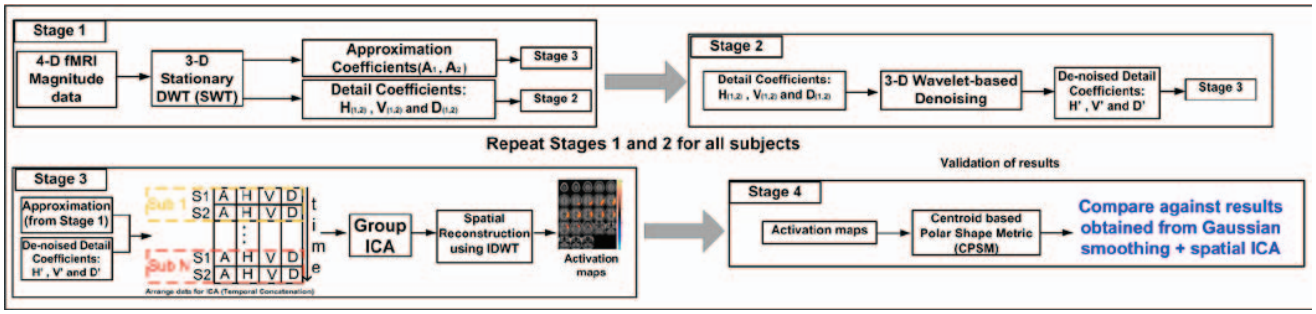


**Figure 1:** Block diagram illustrating the four major stages involved in the proposed wavelet-based fMRI processing framework. Stages 1 and 2 are repeated for all subjects followed by signal separation using group ICA in stage 3 and validation of results in Stage 4.

## 3. RESULTS AND DISCUSSION

It is difficult to estimate the 'ground truth' activation maps for fMRI data due to various obvious reasons. In order to highlight the improvements served by our proposed framework, we present two types of comparisons with the conventional framework (Gaussian smoothing followed by spatial ICA): (1) pseudo-specificity (as there is no ground truth) with focus on contours/edges of the activation regions; and (2) a quantitative comparison using the shape metrics first proposed in [10]. This is the first instance that the centroid-based polar shape metric (CPSM) has been used for comparing shape of activation regions in a real fMRI data set.

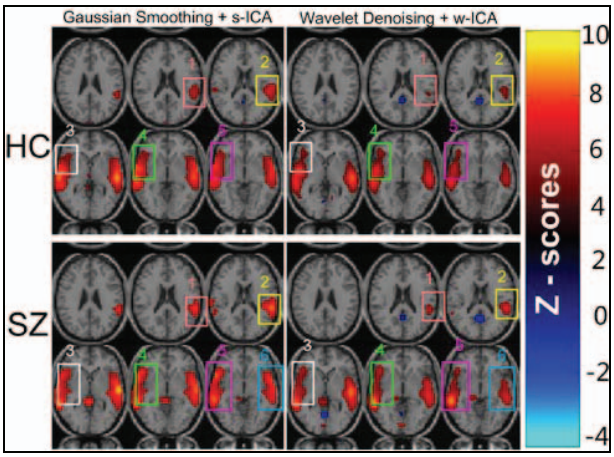


**Figure 2:** Task-positive (auditory) component activation maps (scaled to Z-scores) obtained through a group-ICA of 10 HC and SZ (rows) subjects using the two different frameworks (along columns). The regions of interest (ROIs) are highlighted for emphasis on the difference in shapes and sizes of the activation regions obtained through different methods.

The first point of comparison is presented in Fig. 2 in form of Z-scores computed for the mean activation maps for the task-positive component. Five specific regions of interest (ROI) are highlighted in the HC maps presented for the two methods. The differences can be classified as those in size (ROIs 1 and 2) and shape (ROIs 3, 4 and 5). Similarly, there are six ROIs in the SZ maps (see bottom row in Fig. 2) which highlight differences in size (ROIs 1, 2 and 6) and shape (ROIs 3, 4 and 5) of the activation regions obtained through the two different methods. It is clear from Fig. 2 that the proposed framework (right column in Fig. 2) is able to obtain more specificity where the activations have sharper edges and contours in contrast to circular and smooth edges. In lieu of assuming a ground truth, we utilized activation maps obtained through group ICA on unsmooth fMRI data to obtain a fair idea of actual activation regions. The conventional framework clearly seems to lose specificity because of Gaussian smoothing whereas the proposed framework shows higher specificity in addition to preservation of shape, especially cusp-type edges and sharper contours indication minimal loss of detail.

Intuitively, wavelet-based denoising is expected to preserve edges and other details especially in low resolution data sets. But, ICA on wavelet coefficients served as an added advantage since the data was de-correlated along spatial frequencies and helped ICA obtain maximally independent components. These components clearly have more well-defined activation shapes as compared to the circular Gaussian-type shapes of the activation regions. To further support this statement we present the shape metric results in Fig. 3. The measure utilized here is known as the centroid-based polar shape metric (CPSM) [10]. The mean activation maps for two different methods and different subject groups, parts of which are shown in Fig. 2, are considered as reference images for the estimation of CPSM. Each subject's back-reconstructed maps in each group are then compared with the relevant reference map to obtain the CPSM values. More details on the estimation and parameters of the shape metric may be found in [10].

The CPSM values for the proposed methodology are consistently lower than the conventional method in both groups, as seen in Figs. 3(a) and 3(b). The CPSM value of for HC $_{(sICA\ vs.\ wICA)}$ (= 233.43) is higher than SZ $_{(sICA\ vs.\ wICA)}$ (CPSM = 114.73) which suggests, SZ perform more consistently with respect to each other while performing the task. This is consistent with other studies showing patients

are showing less unique activation patterns. However other shape metrics are needed to more fully characterize the observed differences [16]. The CPSM values mentioned above were derived by comparing the images in left and right columns of Fig. 2(a) and 2(b). Also, knowledge about behavioral data can be complimentary when attempting to understand such trends. Usually SZ subjects are more cautious about performing the tasks diligently as compared to the HC subjects. This may be attributed as one of the reasons for such an observation in addition to this study's small population of subjects.

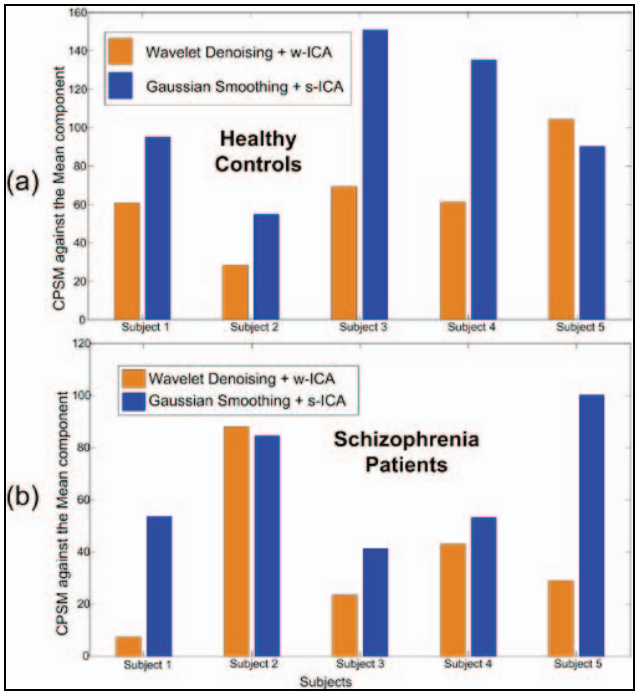


**Figure 3:** Centroid-based Polar Shape Metric (CPSM). Each pair of bars represents the shape difference between the activation map for a subject and the mean activation of that group: (a) Healthy Controls (5 subjects); (b) Schizophrenia patients (5 subjects).

As mentioned above, in contrast to the group data used in this study more interesting differences may be observed when comparing a large group of subjects. This metric may also help in selection of outliers that performed very well and are similar to the mean activation map or performed poorly and are significantly different from the mean activation. One subject from each group can immediately be classified as outliers that have almost equal CPSM values for any analysis method (HC – Subject 5; SZ – Subject 2).

Lastly, it would be interesting to study resting-state networks using the proposed framework in order to obtain more accurate shapes and sizes of the regions functioning as coherent networks in the brain. This might be an initial step towards improving the statistical power in spatial functional connectivity analysis within large groups of subjects.

## 3. CONCLUSION

We presented a new method to analyze multi-group fMRI data and presented enough evidence depicting its superior performance over the conventionally used methods. Also, we presented some other possible applications of the shape metric in analyzing multi-group activation maps.

REFERENCES


[1] K. Friston, A. Holmes, K. Worsley, J. Poline, C. Frith, and R. Frackowiak, "Statistical parametric maps in functional imaging: a general linear approach," *Human Brain Mapping*, vol. 2, (no. 4), pp. 189-210, 1994.

[2] R. Cox, "AFNI: software for analysis and visualization of functional magnetic resonance neuroimages," *Computers and Biomedical Research*, vol. 29, (no. 3), pp. 162-173, 1996.

[3] S. Smith, M. Jenkinson, M. Woolrich, C. Beckmann, T. Behrens, H. Johansen-Berg, P. Bannister, M. De Luca, I. Drobnjak, and D. Flitney, "Advances in functional and structural MR image analysis and implementation as FSL," *NeuroImage*, vol. 23, pp. S208-S219, 2004.

[4] S. Mallat, "A theory for multiresolution signal decomposition: The wavelet representation," *IEEE transactions on pattern analysis and machine intelligence*, vol. 11, (no. 7), pp. 674-693, 1989.

[5] M. Breakspear, M. Brammer, T. Bullmore, P. Das, and L. Williams, "Spatiotemporal wavelet resampling for functional neuroimaging data," *Human Brain Mapping*, vol. 23, (no. 1), pp. 1-25, 2004.

[6] C. Long, E. Brown, D. Manoach, and V. Solo, "Spatiotemporal wavelet analysis for functional MRI," *NeuroImage*, vol. 23, (no. 2), pp. 500-516, 2004.

[7] A. Pizurica, W. Philips, I. Lemahieu, and M. Acheroy, "A versatile wavelet domain noise filtration technique for medical imaging," *IEEE transactions on medical imaging*, vol. 22, (no. 3), pp. 9, 2003.

[8] D. Van De Ville, M. Seghier, F. Lazeyras, T. Blu, and M. Unser, "WSPM: Wavelet-based statistical parametric mapping," *NeuroImage*, vol. 37, (no. 4), pp. 1205-1217, 2007.

[9] A. Wink and J. Roerdink, "Denoising functional MR images: a comparison of wavelet denoising and Gaussian smoothing," *IEEE transactions on medical imaging*, vol. 23, (no. 3), pp. 374-387, 2004.

[10] S. Khullar, A. Michael, N. Correa, T. Adali, S. Baum, and V. Calhoun, "Wavelet-based fMRI analysis: 3-D denoising, signal separation, and validation metrics," *NeuroImage*, 2010.

[11] M. Hilton, T. Ogden, D. Hattery, G. Eden, and B. Jawerth, "Wavelet denoising of functional MRI data," in Wavelets in Medicine and Biology: CRC Press, 1996.

[12] V. Calhoun, K. Kiehl, and G. Pearlson, "Modulation of temporally coherent brain networks estimated using ICA at rest and during cognitive tasks," *Human brain mapping*, vol. 29, (no. 7), pp. 828-838, 2008.

[13] K. Kiehl, K. Laurens, T. Duty, B. Forster, and P. Liddle, "Neural sources involved in auditory target detection and novelty processing: an event-related fMRI study," *Psychophysiology*, vol. 38, (no. 01), pp. 133-142, 2001.

[14] L. Freire, A. Roche, and J. Mangin, "What is the best similarity measure for motion correction in fMRI time series?," *IEEE transactions on medical imaging*, vol. 21, (no. 5), pp. 470-484, 2002.

[15] D. Middleton and R. Esposito, "Simultaneous optimum detection and estimation of signals in noise," *IEEE transactions on information theory*, vol. 14, (no. 3), pp. 10, 1968.

[16] V.D. Calhoun, T. Adali, K.A. Kiehl, R.S. Astur, J.J. Pekar, and G.D. Pearlson, "A Method for Multi-task fMRI Data Fusion Applied to Schizophrenia," *Human Brain Mapping*, vol. 27, pp. 13, 2006.